Short communication

Carbon–fiber–silicon-nanocomposites for lithium-ion battery anodes by microwave plasma chemical vapor deposition

H. Wolf*, Z. Pajkic, T. Gerdes, M. Willert-Porada

University of Bayreuth, Universitaetsstrasse 30, 95447 Bayreuth, Germany

ARTICLE INFO

ABSTRACT

The paper presents a new synthesis method for nanocomposites made from amorphous and nanocrystalline silicon deposited on a carbon fiber substrate and the Li-ion battery anode performance results achieved with such nanocomposites.

Atmospheric microwave plasma coating enables deposition of nanosized silicon onto the 3D-carbon fiber substrate containing graphite as filler. The microstructure and composition of the nanocomposites is characterized by means of XRD, SEM, Raman spectroscopy and N_2 gas adsorption. Amorphous silicon and nanocrystalline silicon act together with the graphitic carbon as Li-intercalation material. Excellent adhesion to the "electrical network" provided by the carbon fibers is observed. In half-cell measurements versus lithium, a stable capacity is found even at multiple cycling with high charge/discharge current. Anodes for Li-ion batteries made from the new material have the potential to significantly increase the reversible capacity of the battery.

For example, more than $700\,\mathrm{mAh\,g^{-1}}$ is obtained for a composite with a silicon content of less than 20 wt.%. The irreversible specific capacity is comparable to the one of an unmodified carbon fiber substrate.

© 2008 Elsevier B.V. All rights reserved.

1. Introduction

During the past decade, secondary lithium-ion batteries have become the major power source for mobile applications, such as cellular phones, digital cameras and notebooks. Their rather high energy density of up to $120\,\mathrm{Wh\,kg^{-1}}$ makes Li-ion-batteries superior to other battery types for mass market applications (e.g. lead-acid batteries: $30\,\mathrm{Wh\,kg^{-1}}$; Nickel-metal-hydride batteries: $\sim 80\,\mathrm{Wh\,kg^{-1}}$).

State-of-the-art anodes of Li-ion batteries usually consist of graphite powder, in which lithium ions can be intercalated and de-intercalated [1]. Mechanical stability is provided by a polymeric binder, usually PVDF [2]. Besides graphite, which possesses a theoretical specific capacity of $372\,\mathrm{mAh\,g^{-1}}$, there are several other promising materials for application as anode material in Li-ion batteries, with theoretical specific capacities superior to graphite, like tin [3] and silicon. Unlike graphite, where lithium-ions are stored in between the graphene layers in the graphite lattice during intercalation [4], silicon forms binary alloys with lithium [5]. A structure of up to $\mathrm{Li_{4.4}Si}$ is reported [6], resulting in a theoretical specific capacity of $4200\,\mathrm{mAh\,g^{-1}}$. Unfortunately, the alloying comes along with

a significant volume change of around 300% [7], which leads to high mechanical stresses, and, upon repeated cycling, to fast disintegration of the material and a very high irreversible capacity. In addition, the poor electrical conductivity of silicon (only $250\,\mathrm{\mu S\,m^{-1}}$) leads to heat generation upon cycling due to the high internal resistance and limits the applicable charge current.

Intense research activities are currently undertaken in the field of carbon–silicon composites [8–10]. This group of materials seems to be a promising solution to overcome the silicon related problems discussed above.

By using nanostructured silicon in the composites, mechanical stresses arising from volume changes will decrease, which leads to a reduced irreversible specific capacity. Such nanostructured materials can be prepared by e.g. ball-milling [11]. But upon prolonged cycling, capacity fading due to loss of electrical contact can still be detected. Superior performance could be expected, if a good adhesion between the carbon and the nanostructured silicon would exist.

By means of chemical vapor deposition (CVD), nanostructured materials can be deposited on a suitable substrate. In previous work at the University of Bayreuth, metals as well as metal nitrides and carbides were successfully deposited on various carbon substrates by microwave-assisted atmospheric pressure CVD [12,13].

In the presented work, nanostructured silicon was deposited on a commercial 3D-carbon fiber substrate. Aim of the work is to obtain
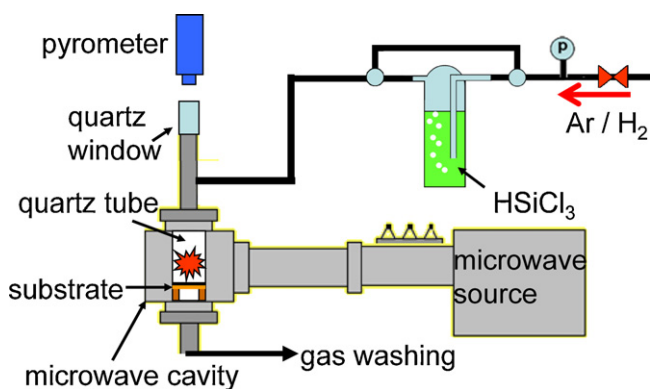

Fig. 1. Experimental setup for CVD of silicon on carbon fiber substrate in microwave plasma CVD reactor.

a composite, in which the carbon fibers provide a high surface area for deposition of nanosized silicon, as well as mechanical stability and electrical conductivity by their percolating network. The deposited silicon as well as the graphitic part of the carbonaceous substrate act as intercalation material.

2. Experimental

The microwave assisted CVD experiments were carried out in an in-house built microwave plasma reactor at atmospheric pressure in an argon-hydrogen atmosphere. A schematic drawing of the experimental setup is given in Fig. 1.

As carbonaceous substrate, a commercial gas diffusion layer (GDL10AA, SGL, Germany) was used. This material consists of carbon fibers and graphite particles, which are attached to the fibers at and near to junctions in order to enhance the electrical conductivity. Trichlorsilane (TCS) was employed as silicon precursor. Before starting the CVD process, the setup was purged with argon-hydrogen (5% H_2) for at least 30 min. Following to purging, the argon-hydrogen gas stream was reduced to 0.04 $m^3 h^{-1}$, and microwave plasma was ignited. Typical microwave power during the experiments was 1 kW. After the substrate had reached the processing temperature of 900 °C, the argon-hydrogen gas was re-routed through the TCS supply. The high vapor pressure of TCS at room temperature enables

sufficient transport with the carrier gas stream. When entering the plasma zone, the precursor is decomposed and silicon is deposited on the substrate. Other gaseous decomposition products (like HCl, $SiCl_2$ and $SiCl_3$) are neutralized in alcoholic NaOH solution.

TCS was added for varying processing times between 30 s and 5 min. After that time, the precursor-supply was disconnected and the microwave source was turned off. In order to remove decomposition products of the TCS, the argon hydrogen gas stream was increased to 0.12 $m^3 h^{-1}$. The reactor was cooled down to room temperature under constant purging before removing the sample.

The silicon content was measured gravimetrically. Crystalline phases of the composite material are determined by means of XRD. Primary crystallite size was calculated by the Rietveld method. SEM images were taken to investigate the morphology and surface structure of the samples. Raman spectroscopy allowed the determination of amorphous and crystalline silicon. Specific surface area was measured by N_2 gas adsorption (BET method).

For investigation of electrochemical properties, half-cell measurements with lithium metal as cathode are performed. A 12 mm diameter disc of the composite material was punched out and directly used for testing, without additional binder. The cells were assembled in a glovebox under argon (H_2O < 1 ppm, O_2 < 40 ppm), using 1 M $LiPF_6$ in 1:1 mixture of ethylene carbonate and ethyl-methyl-carbonate as electrolyte and a Whatman® GF-C glass fiber separator. The half cells were cycled galvanostatically between 2 V and 0.5 mV, with varying current from $C/20$ to up to 2 C. Additionally, the specific electrical conductivity of the composites was measured by electrochemical impedance spectroscopy.

3. Results

SEM images show, that a porous Si coating has been formed on the carbonaceous substrate during the CVD-process. The coating consists of numerous small particles of quite homogeneous size, grown together into agglomerates. Fig. 2 shows SEM-images of three composites prepared with different coating time. The Si agglomerates size is increasing with prolonged coating time. After 1 min, the mean agglomerate size derived from SEM images lies between 100 and 150 nm. After 2.5 min coating time the agglomerates have growth to a size between 250 and 500 nm, whereas after 5 min coating duration the Si-agglomerates have already reached
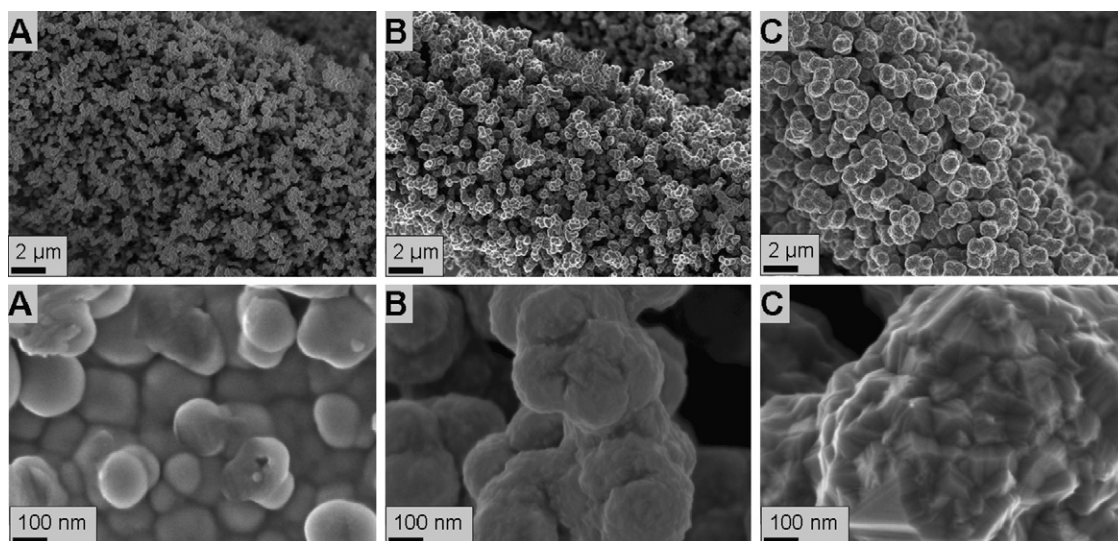

Fig. 2. SEM-images of three carbon–silicon-composites, prepared with different coating time. Overview of coated fibers (top) and high resolution images of deposited silicon particles (bottom). Coating time: A = 1 min; B = 2.5 min; C = 5 min. Longer coating time leads to larger silicon particles.
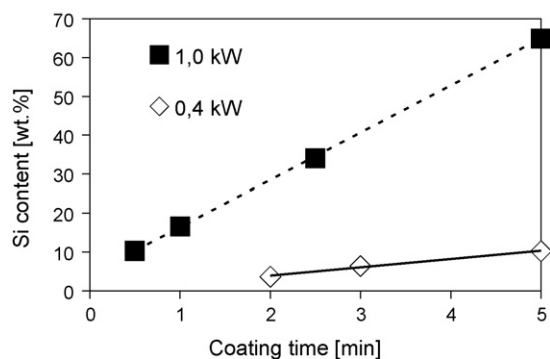
Fig. 3. Silicon content of the carbon silicon composite materials depending on the CVD processing time at 1 kW and 0.4 kW microwave power, respectively.

Fig. 5. Specific electrical conductivity σ depending on CVD coating time. The triangle indicates the unmodified carbon fiber substrate, which shows higher conductivity than the composite materials.

μm size. XRD scans revealed elemental silicon as well as ordered carbon and graphite in the composites. Only traces of SiC were detected. The SiC content as well as the primary crystallite size of the deposited silicon were determined by the Rietveld method. The primary crystallite size of the silicon was found to be around 27 nm for all materials, whereas the calculated SiC content varies between 0.3 and 2.5%.

Raman spectroscopy measurements revealed the composition of the coating to be crystalline silicon and mixtures of amorphous and crystalline silicon, respectively. The composition is depending on the coating time and is varying over the sample volume. Directly on the amorphous carbon fibers, mainly amorphous silicon can be detected, whereas crystalline silicon is found on the graphite particles of the substrate. After a coating time of more than 2.5 min at a power level of 1 kW microwave power, only crystalline silicon can be detected.

The silicon content of the composite materials was found to increase linearly with increasing duration of the CVD process. The deposition rate is strongly dependent on the microwave power used to sustain the plasma. Fig. 3 shows the silicon content for several composites, depending on microwave power and coating time.

The specific surface area of the composites was found to decrease with increasing duration of the CVD process. Results for several composites prepared at 1 kW microwave power are given in Fig. 4.

The specific electrical through-plane conductivity of the composites is decreasing exponentially with increasing silicon content, due to the low electrical conductivity of the deposited silicon. The results for the plain substrate and five composite materials, prepared at 1 kW microwave power are given in Fig. 5.
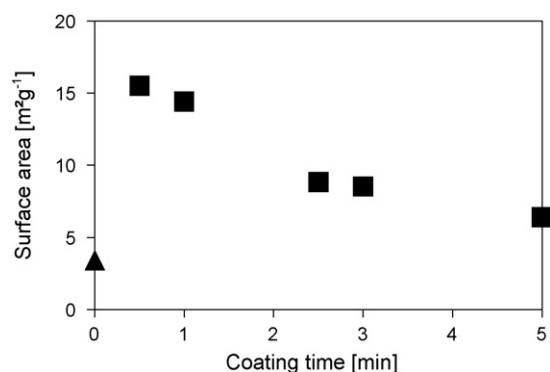
Despite the low electrical conductivity, composite materials with a silicon content of less than 35 wt.% were found to show good electrochemical performance in half-cell measurements vs. lithium at small charge/discharge currents. Fig. 6 shows results for several cells with different silicon content, compared to the results obtained with the unmodified carbon fiber substrate. The irreversible capacity of the composite materials is comparable to c_{irr} of the substrate, whereas the absolute reversible capacity is increased significantly with increasing silicon content.

For a silicon content of 20 wt.% or less, stable capacity was obtained also for higher charge/discharge currents of up to 2 C, as shown in Fig. 7.

4. Discussion

The increase of silicon agglomerate size with increasing coating time is considered to be due to sintering. The substrate temperature of 900 °C is sufficient to obtain a fast sintering of the primary particles of the deposited nanosized silicon, the effect was found to be reproducible in post-deposition heat treatment performed in an conventional tubular furnace at similar substrate temperature.

At 900 °C, also crystallization of the deposited silicon is enhanced [14], which explains, why amorphous silicon can only be found in nanocomposites processed with short coating times.

The primary crystallite size of the silicon derived from Rietveld method is almost the same for all carbon–silicon composites, as the

Fig. 4. Specific surface area depending on the coating time at 1 kW microwave power. The triangle at 0 min indicates the unmodified carbon fiber substrate.
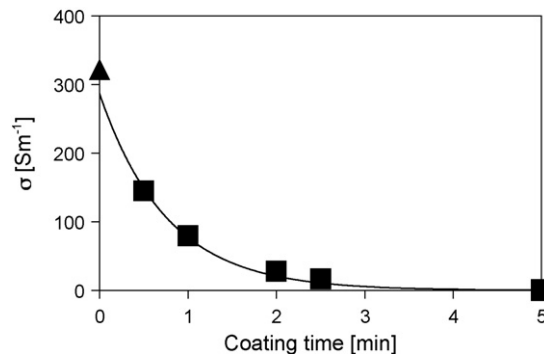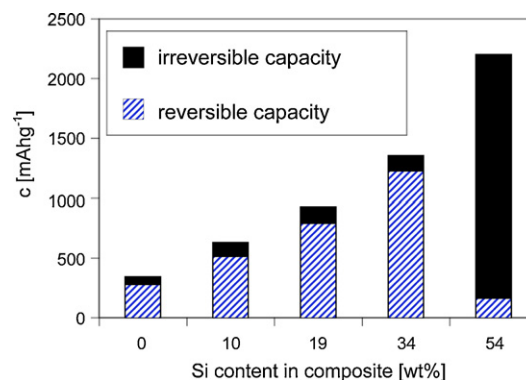

Fig. 6. First cycle reversible and irreversible specific capacity in dependence of silicon content at a charge/discharge current of $C/20$. Up to a silicon content of 34 wt%, the carbon–silicon-composites are clearly superior compared to the carbonaceous substrate. Reversible specific capacity is more than 1200 mAh g^{-1} for the 34 wt% sample.
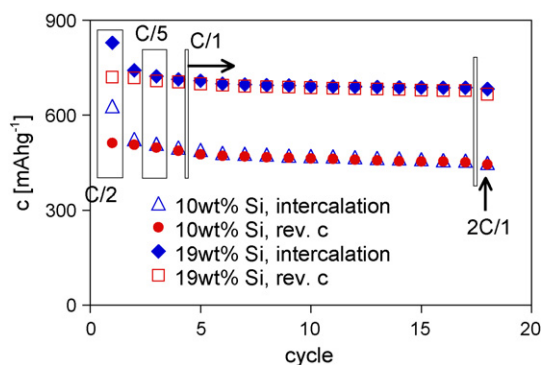
Fig. 7. 18 cycles of intercalation and de-intercalation at increasing current for two carbon–silicon-composites with a silicon content of 10 and 19 wt.%, respectively. A stable reversible specific capacity is observed for both materials up to a current of 2 C.

duration of temperature exposure is too short to affect it. Dutta et al. [14] reported similar results when investigating the crystallization of silicon.

The decrease of the specific surface area with increasing coating time is also due to effects of sintering within agglomerates, as surface area is dependent on agglomerate porosity. The larger the number of voids within agglomerates, the larger is the surface in relation to its mass.

Formation of SiC is possible at 900 °C [15], but the reaction is quite slow, therefore only a small amount can be detected in the composites by means of XRD.

The small amount of SiC that forms between the substrate and the coating due to reaction of the carbon with the deposited silicon during the process is considered to enhance the stability of the composite during electrochemical cycling, as the deposited silicon is not only mechanically but also chemically bonded to the substrate.

The electrical through-plane conductivity is decreased exponentially with coating time, as the silicon is located at the surface of the carbonaceous structure. Therefore, also a thin layer of silicon can decrease the through-plane conductivity of the composite drastically, because the contact resistance towards the electrodes of the measurement unit is increased.

For a silicon content of 54 wt%, achieved after a coating time of 5 min, c_{irr} was found to be more than 90%. The large, μm sized silicon agglomerates of this composite obviously disintegrated during the intercalation step, therefore the electrical contact to the substrate was lost. The composite obtained with 2.5 min coating time, containing 34 wt% Si only, showed good properties at small
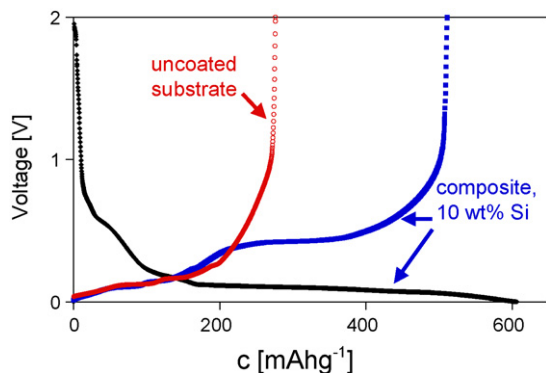
charge/discharge currents. A c_{irr} of less than 10% was obtained, indicating, that the silicon structure has not disintegrated and is still connected to the carbon substrate. An increased current of $C/2.5$ lead to cell failure during de-intercalation. This might be explained by this composites low electrical through-plane conductivity of only 16 S m^{-1}.

According to Khomenko and Barsukov [16], the reversible specific capacity of a component in a composite material can be calculated, if de-intercalation behavior and content of the other components are known. For a silicon content of less than 35 wt%, the reversible specific capacity of Si in the first cycle at $C/20$ was found to be between 2.5 Ah g^{-1} and more than 3 Ah g^{-1}.

Voltage plotted over specific capacity reveals, that lithium is de-intercalated from both the silicon and the carbonaceous substrate. Fig. 8 shows the first cycle of intercalation and de-intercalation for a composite containing 10.2 wt.% silicon. The curve shows characteristic voltage plateaus for de-intercalation from carbonaceous material (range 25–250 mV) and in addition a pronounced plateau at around 400 mV, indicating the lithium extraction from a lithium–silicon alloy. The addition of 10.2 wt.% nanostructured silicon by CVD almost doubled the reversible specific capacity, as compared to the uncoated substrate.

5. Conclusion

A new carbon–silicon-nanocomposite material was prepared in an atmospheric microwave plasma CVD process. High reversible specific capacity even at high charge/discharge currents has been achieved in half-cell measurements.

Further work will concentrate on optimization of the long-term stability of the composite material over several 100 cycles at high current, as well as the behavior at elevated temperatures. Also, CVD process parameters will be varied in order to achieve high silicon loading while maintaining a small Si-agglomerate size.

Acknowledgements

References

[1] D. Aurbach, Y. Talyosef, B. Markovsky, E. Markevich, E. Zinigrad, L. Asraf, J.S. Gnanaraj, H.-J. Kim, Electrochim. Acta 50 (2004) 247–254.
[2] H.-Q. Li, R.-L. Liu, D.-Y. Zhao, Y.-Y. Xia, Carbon 45 (2007) 2628–2635.
[3] H. Zhao, C. Jiang, X. Hea, J. Rena, C. Wan, Electrochim. Acta 52 (2007) 7820–7826.
[4] R. Yazami, P. Touzain, J. Power Sources 9 (1983) 365–371.
[5] W.J. Weydanz, M. Wohlfahrt-Mehrens, R.A. Huggins, J. Power Sources 81–82 (1999) 237.
[6] T. Hasegawa, S.R. Mukai, Y. Shirato, H. Tamon, Carbon 42 (2004) 2573–2579.
[7] M. Holzapfel, H. Buqa, W. Scheifele, P. Novak, F.-M. Petrat, Chem. Commun. (2005) 1566–1568.
[8] J. Xie, G.S. Cao, X.B. Zhao, Mater. Chem. Phys. 88 (2004) 295–299.
[9] M. Yoshio, T. Tsumura, N. Dimov, J. Power Sources 146 (2005) 10–14.
[10] X.-W. Zhang, P.K. Patil, C. Wang, A.J. Appleby, F.E. Little, D.L. Cocke, J. Power Sources 125 (2004) 206–213.
[11] Y. Zheng, J. Yang, J. Wang, Y. NuLi, Electrochim. Acta 52 (2007) 5863–5867.

Fig. 8. Insertion and extraction of lithium in a composite with 10.2 wt% silicon content at a current of $C/20$ in comparison to de-intercalation from unmodified substrate.

[12] R. Tap, M. Willert-Porada, IEEE Trans. Plasma Sci. 32 (2004) 2085–2092.
[13] H. Wolf, Z. Pajkic, M. Willert-Porada, Adv. Sci. Technol. 45 (2006) 851–856.
[14] J. Dutta, I.M. Reaney, C. Bossel, R. Houriet, H. Hofmann, NanoStructured Mater. 6 (1995) 493–496.
[15] C.K. Chung, B.H. Wu, T.S. Chen, C.C. Peng, C.W. Lai, Thin Solid Films (2007), doi:10.1016/j.tsf.2007.06.226.
[16] V.G. Khomenko, V.Z. Barsukov, Electrochim. Acta 52 (2007) 2829–2840.
[17] J. Thiessen, M. Bensch, S. Aschauer, Neuartiges Anodenmaterial für sekundäre Lithium Ionen-Batterien, Student Thesis, University of Bayreuth, 2007.